Elsevier Editorial System(tm) for Water Research
Manuscript Draft

Manuscript Number:

Title: Operational, design and microbial aspects related to power production with microbial fuel cells implemented in constructed wetlands

Article Type: Research Paper

Keywords: constructed wetlands; domestic wastewater; microbial fuel cells; Geobacter

Corresponding Author: Prof. Jaume Puigagut,

Corresponding Author's Institution: Technical University of Catalunya

First Author: Clara Corbella

Order of Authors: Clara Corbella; Miriam Guivernau; Marc Viñas; Jaume Puigagut

Abstract: This work aimed at determining the amount of energy that can be harvested by implementing microbial fuel cells (MFC) in horizontal subsurface constructed wetlands (HSSF CWs) during the treatment of real domestic wastewater. To this aim, MFC were implemented in a pilot plant based on two HSSF CW, one fed with primary settled wastewater (Settler line) and the other fed with the effluent of a hydrolytic up-flow sludge blanket reactor (HUSB line). The eubacterial and archaeal community was profiled on wetland gravel, MFC electrodes and primary treated wastewater by means of 16S rRNA gene-based 454-pyrosequencing and qPCR of 16S rRNA and mcrA genes. Maximum current (219 mA/m2) and power (36 mW/m2) densities were obtained for the HUSB line. Power production pattern correlated well with water level fluctuations within the wetlands, whereas the type of primary treatment implemented had a significant impact on the diversity and relative abundance of eubacteria communities colonizing MFC. It is worth noticing the high predominance (13-16% of relative abundance) of one OTU belonging to Geobacter on active MFC of the HUSB line that was absent for the settler line MFC. Hence, MFCs show promise for power production in constructed wetlands receiving the effluent of a HUSB reactor.

Suggested Reviewers: Amelia-Elena Rotaru
Department of Microbiology, University of Massachusetts, Amherst, USA
arotaru@microbio.umass.edu

Asheesh Kumar Yadav
Department of Civil and Environmental Engineering, Princeton University, Princeton, NJ 08544, USA
ayadav@princeton.edu

Jose Villaseñor
Chemical Engineering Department, Institute for Chemical and Environmental Technology (ITQUIMA), University of Castilla-La Mancha, Avenida Camilo José Cela S/N, 13071 Ciudad Real, Spain
Jose.Villasenor@uclm.es

Gemma Reguera
Dep. Microbiology and Molecular Genetics Biomedical & Physical Sciences bld. 567 Wilson Road, Rm. 6190 Michigan State University East Lansing, MI 48824

reguera@msu.edu

Highlights

- Cell voltage followed a daily pattern consistent with water level variation.
- Maximum current and power densities were that of 219 mA/m^2 and 36 mW/m^2.
- The primary treatment affected the diversity of bacteria colonizing MFCs.
- The primary treatment affected the relative abundance of bacteria colonizing MFCs.
- A high predominance of one OTU belonging to *Geobacter* was found in anodes biofilm.

Graphical Abstract (for review)

CONSTRUCTED WETLAND TREATMENT PLANT

(1. Homogenization tank; 2. HUSB reactor; 3. Settlers;
4 and 5. Horizontal Subsurface Constructed Wetlands)

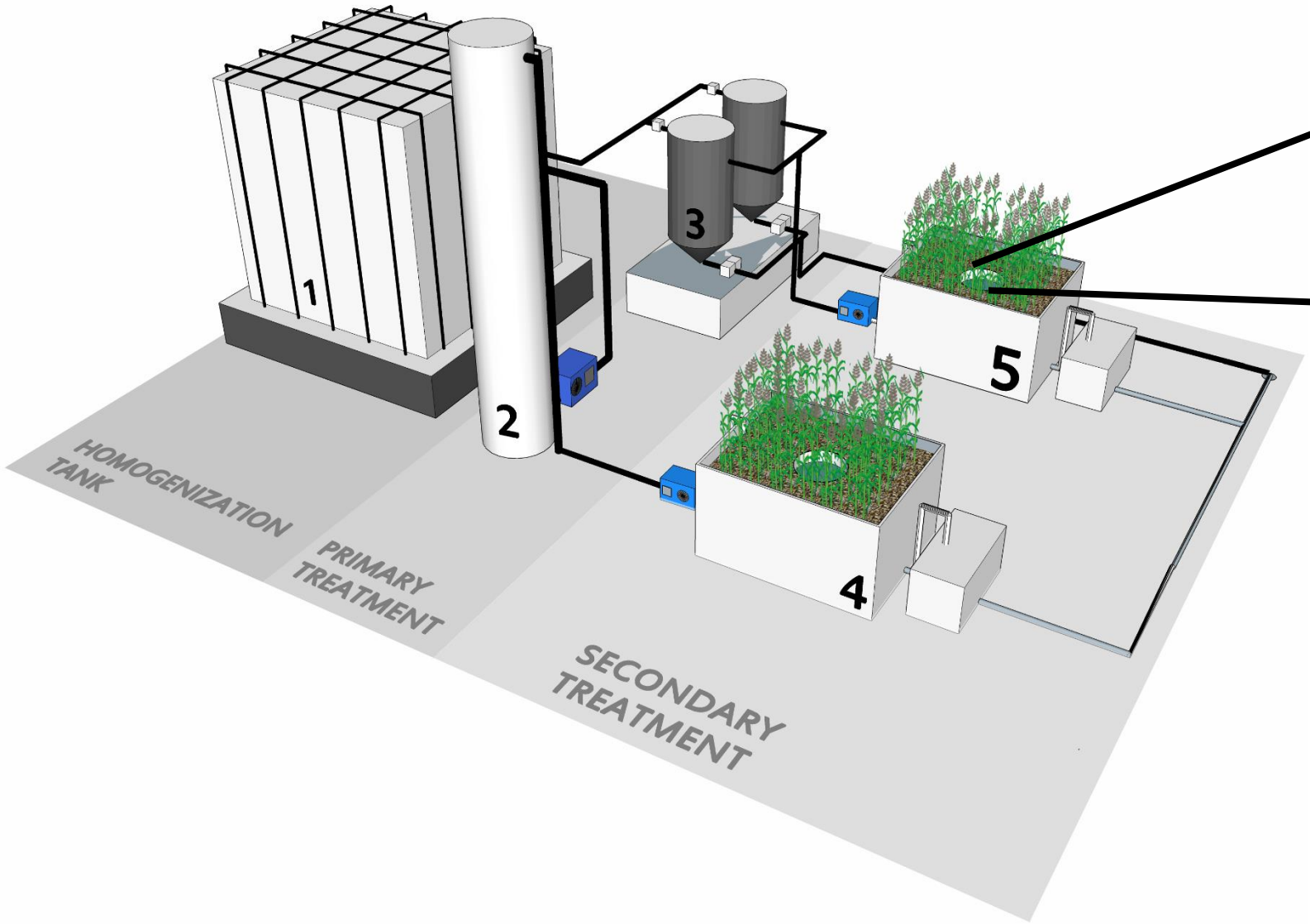

CONSTRUCTED WETLAND MICROBIAL FUEL CELLS

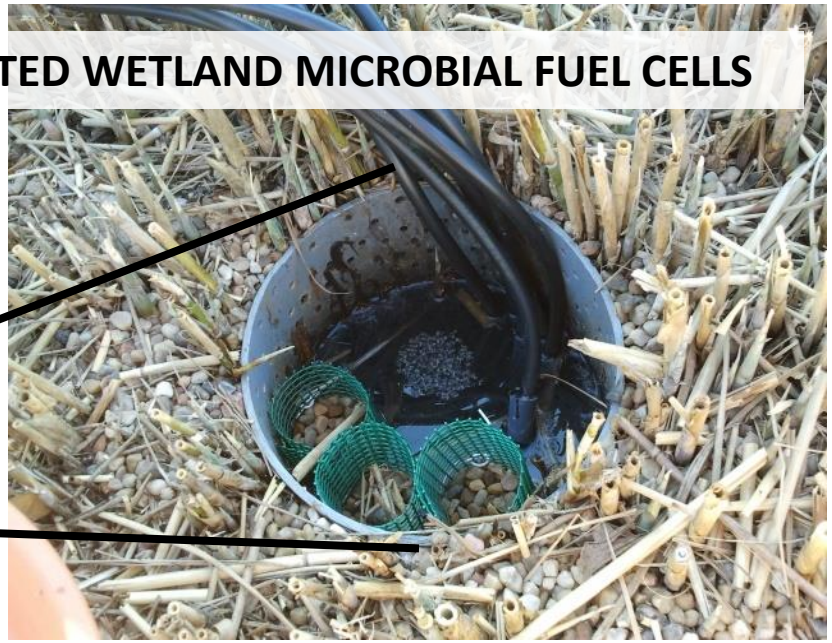

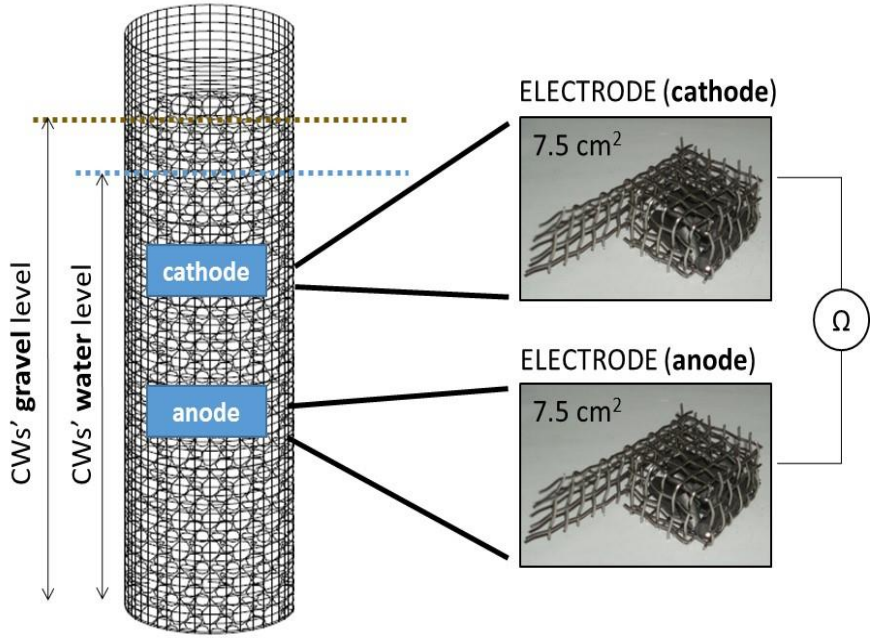

Operational, design and microbial aspects related to power production with microbial fuel cells implemented in constructed wetlands

Clara Corbella[1] , Miriam Guivernau[2], Marc Viñas[2] and Jaume Puigagut[1*]

[1] GEMMA. Department of Hydraulic, Maritime and Environmental Engineering, Universitat Politècnica de Catalunya, c/ Jordi Girona 1-3, Building D1, E-08034 Barcelona, Spain.

[2] GIRO Joint Research Unit IRTA-UPC, IRTA, Torre Marimon, 08140 Caldes de Montbui, Barcelona, Spain.

[*] Corresponding author:

Tel: +0034 934010898

Group of Environmental Engineering and Microbiology (GEMMA)
Polytechnic University of Catalunya - BarcelonaTech
C/Jordi Girona 1-3
08034 Barcelona - Spain

E-mail address: jaume.puigagut@upc.edu

Abstract

This work aimed at determining the amount of energy that can be harvested by implementing microbial fuel cells (MFC) in horizontal subsurface constructed wetlands (HSSF CWs) during the treatment of real domestic wastewater. To this aim, MFC were implemented in a pilot plant based on two HSSF CW, one fed with primary settled wastewater (Settler line) and the other fed with the effluent of a hydrolytic up-flow sludge blanket reactor (HUSB line). The eubacterial and archaeal community was profiled on wetland gravel, MFC electrodes and primary treated wastewater by means of 16S rRNA gene-based 454-pyrosequencing and qPCR of *16S rRNA* and *mcrA* genes. Maximum current (219 mA/m^2) and power (36 mW/m^2) densities were obtained for the HUSB line. Power production pattern correlated well with water level fluctuations

within the wetlands, whereas the type of primary treatment implemented had a significant impact on the diversity and relative abundance of eubacteria communities colonizing MFC. It is worth noticing the high predominance (13-16% of relative abundance) of one OTU belonging to *Geobacter* on active MFC of the HUSB line that was absent for the settler line MFC. Hence, MFCs show promise for power production in constructed wetlands receiving the effluent of a HUSB reactor.

Key words: constructed wetlands, domestic wastewater, microbial fuel cells, *Geobacter*

1 Introduction

Microbial Fuel Cells (MFCs) are bioelectrochemical systems that generate current by means of electrochemically active microorganisms as catalysts. In a MFC, organic and inorganic substrates are oxidized by bacteria and the electrons are transferred to the anode from where they flow through a conductive material and a resistor to a higher redox electron acceptor, such as oxygen, at the cathode (Logan et al., 2006, Rabaey et al., 2007). So far, there are two well-known bacterial genera which present exoelectrogenic activity in pure culture, i.e., *Shewanella (*Ringeisen et al., 2006) and *Geobacter* (Richter et al., 2008; Kiely et al., 2011). To date, a high diversity of microorganisms has been described to perform anode respiration to a certain degree (Logan, 2009). Over 20 different exoelectrogenic bacteria have been reported in the last decade, belonging to diverse phylogenetic groups: alpha-proteobacteria (*Rhodopseudomonas, Ochrobactrum* and *Acidiphilium*), beta-proteobacteria (*Rhodoferax, Comamonas*), gamma-proteobacteria (*Shewanella, Pseudomonas, Klebsiella, Enterobacter and Aeromonas, Citrobacter*), delta-proteobacteria (*Geobacter*, *Geopsychrobacter, Desulfuromonas* and *Desulfobulbus*), Epsilon-proteobacteria (Arcobacter), Firmicutes (*Clostridium* and *Thermincola*), Acidobacteria (*Geothrix*) and Actinobacteria (*Propionibacterium*) (Logan 2009; Xing et al., 2010). However, the power density achieved in most of the experiments working with mixed cultures is higher than in pure cultures (Rabaey & Verstraete, 2005; Rabaey, et al., 2004; Nevin et al., 2008). These results reinforce the idea that increased electricity generation could be attributed to synergistic interactions within the microbial community. Namely, there could be microorganisms that do not exchange directly electrons with the electrode, but could be settling up interactions among other members

of the microbial community playing a crucial role not only in the operation of a MFC but also on its performance improvement (specially under the presence of complex organic substrates such as wastewater) (Borole et al., 2011 and references therein). Methanogens such as *Methanosaeta* and *Methanosarcina* are, for example, routinely detected in mixed species, anode biofilms of MFCs, where they presumably promote syntrophic interactions with exoelectrogenic eubacteria in the anode biofilm (Chung and Okabe, 2009; Rotaru et al., 2014a, 2014b; Sotres et al., 2014).

Compounds oxidized at the anode are mainly simple carbohydrates such as glucose or acetate that can be already present in the environment or obtained from the microbial degradation of complex organic substrates such as organic sediments or wastewater (Min and Logan, 2004; Reimers et al. 2001, Rabaey and Verstraete, 2005). MFCs are, therefore, an alternative technology to harvest energy directly from wastewater in the form of electricity (Du et al., 2007). In order to ensure the use of the anode as the final electron acceptor by electrochemical active microorganisms, no acceptor with higher redox potential shall be present in their vicinity (Lefebvre et al., 2011). Consequently, the electromotive force of the cell will depend on the redox gradient between the anode and the cathode (Logan et al. 2006, Rabaey and Verstraete, 2005).

To generate the redox gradient between electrodes, MFCs require two separated areas that contain the anode (anaerobic area) and the cathode (aerobic area). In some aquatic environments there is the existence of natural redox gradients that can be exploited to produce energy via MFC implementation. So far, MFC have been mostly implemented in rice paddy fields (De Schamphelaire et al.., 2008, Kaku et al., 2008) or marine sediments (Reimers et al.., 2001; Rezaei et al., 2007). Furthermore, horizontal subsurface flow constructed wetlands (HSSF CWs) are engineered systems used for wastewater treatment that are subjected to great spatial redox variations (especially in depth) (García et al. 2003). Although the system is mainly anaerobic (Baptista et al. 2003), the very upper part of the wetland remains under aerobic conditions because its close contact with the atmosphere giving redox gradients of about 0.5 V (García et al. 2003; Dusek et al. 2008; Pedescoll et al. 2013; Corbella et al., 2014). As a result, natural redox gradients in HSSF CWs could be exploited to produce energy via MFC implementation, though only laboratory or small-scale based experiments with synthetic wastewater are currently available (Yadav et al., 2012, Villaseñor et al., 2013; Fang et al., 2013; Zhao et al., 2013). Furthermore, one of the main problems of constructed wetlands is clogging (Pedescoll et al. 2011a). To prevent it, primary treatments are

applied to wastewater. Generally, physical treatments such as settlers or imhoff tanks are used. However, recently other technologies such as hydrolytic upflow sludge blanket (HUSB) reactors are being considered (Pedescoll et al. 2011b). A HUSB reactor prevents methane formation during organic matter hydrolysis due to a low HRT when compared to conventional anaerobic digesters (Ligero et al., 2001). Moreover, HUSB reactors have the advantage over conventional settling of providing a higher concentration of biodegradable substrates (such as acetate) (Gonçalves et al., 1994) that can be easily removed in HSSF CWs. HUSB reactors as a primary treatment are of special interest in the context of MFC implemented in HSSF CW. Accordingly, HUSB reactors will provide a higher concentration of rapidly biodegradable substrate when compared to conventional settling, thus providing higher amount of fuel for MFC. This work aimed at determining the amount of energy that can be harvested by implementing MFC in HSSF CW during the treatment of real domestic wastewater. The effect of the type of primary treatment on power production, the daily and seasonal pattern of power production and the assessment of microbial populations associated to wastewater, electrodes (graphite) and CW materials (gravel) are also addressed.

2 Material and methods

2.1 Pilot plant

The pilot plant used in this study consisted of two horizontal subsurface flow constructed wetland. The wetlands were set up in March 2011 and had 0.4 m^2 of surface (70 cm length x 55 cm width). Wetlands were filled up with gravel (D_{60}=7.3; C_u=0.8) giving an initial porosity of 40%. Water level within the wetlands was kept at 30 cm (5 cm below the gravel surface). Both wetlands were planted with common reed (*Phragmites australis*), which were very mature at the moment this study was conducted (2.5 years after wetlands construction). Each wetland had a PVC cylinder of 20 cm diameter placed at the middle of the wetland that served not only to sample extraction but also to allocate the MFC.

The pilot plant was fed with urban wastewater pumped directly from the municipal sewer. Initially, wastewater was coarsely screened and after that it was pumped to a homogenisation tank of 1.2 m^3 where wastewater was continuously stirred in order to avoid solids sedimentation. After the homogenisation tank, wastewater was conveyed to the primary treatment. The primary treatment consisted of conventional settling for one

of the wetlands and an anaerobic treatment based on a hydrolytic up-flow sludge blanket reactor (HUSB reactor) for the other. The HUSB reactor consisted of a PVC cylinder of 115 L of volume that was operated at 4 hours of HRT and at 10 g VSS/L. The settler consisted of two PVC cones of 14 L volume each that were operated in parallel. After the primary treatment, wastewater was pumped to the wetlands at a flow rate of 21 L/day, giving a design HRT of 2.6 days and an organic loading rate of 7.2 $g.BOD_5.m^{-2}.day^{-1}$ and 6 $g.BOD_5.m^{-2}.day^{-1}$ to the HUSB and Settler line, respectively.

2.2 Microbial fuel cells

Six MFC were set up for the purposes of the present work. Three of them were placed within the wetland fed by a HUSB reactor (HUSB_MFCs) and the rest of them were placed within the wetland fed by the settler (SET_MFCs) (Figure 1). Two of the three MFC for each wetland were in closed circuit whereas the other was left in open circuit and served as a control.

Each cell consisted of a cylinder of 40 cm in length and 5 cm in diameter made out of a plastic mesh filled with gravel up to a height of 35 cm (Figure 2). Both electrodes, anode and cathode, were placed within the cylinder at 15 cm and 5 cm below the water level, respectively. Thus, the distance between electrodes was that of 10 cm.

The anode and cathode were made out of 20 cylindrical graphite rods (1 cm length and 0.5 cm diameter each) wrapped with a stainless steel mesh marine grade 316L. Electrodes were 2.5 cm length, 3 cm wide and 1 cm height and square shaped (Figure 2). The external circuit connected both electrodes by cooper wires and one external resistance of 1000 ohms. Epoxy resins were used to isolate connections from water.

2.3 Redox, conductivity, temperature and water level measurements

Redox potential, water temperature, conductivity and water level were monitored all through the experiment. Redox potential was measured by means of an ORP probe (Ag/AgCl reference system - accuracy: ± 10 mV). Water level variation within the wetlands was determined using a pressure probe (TNS 119, Desin Instruments SA). Water temperature was measured using a Campbell Scientific 107-L Temperature Sensor. Finally, water conductivity was measured using a portable probe (Endress+Hauser CLM381). Water level variation and temperature were continuously measured while redox was alternatively measured in each wetland during periods of

158 approximately 4 days. Both parameters were recorded by connecting the sensors to
159 dataloggers (Datataker DT50 series 3) that stored one value every 15 minutes.
160 Conductivity and pH were manually measured three times a week. Regarding redox
161 potential measurement, two probes were placed just by the electrodes (at 5 cm (cathode)
162 and 15 cm (anode) depth) and data obtained was transformed to express results in terms
163 of the standard hydrogen electrode (E_H).

164 *2.4 Voltage measurements*

165 MFC were connected to a datalogger (Datataker DT50 series 3) which collected a value
166 of voltage across the external resistance every 15 minutes. Voltage measurements were
167 conducted in both lines from middle February to middle June 2013 (first period). After
168 that, only the HUSB line was kept in operation until the end of the study period in July
169 2013 (second period).

170 *2.5 Physical and chemical analyses*

171 Water quality parameters surveyed during the experiment were BOD_5, total COD,
172 soluble COD, ammonia, nitrate, nitrite, sulphate and orthophosphate. Analyses were
173 performed according to Standard Methods (APHA-AWWA-WEF, 2005). Sampling was
174 conducted at the inlet, middle and outlet of the wetlands on a weekly basis. Water flow
175 was also daily measured and removal efficiencies calculated on a mass balance basis.

176 *2.6 Electrochemical characterization*

177 Cell electromotive force was calculated according to Logan et al. (2006). Current was
178 calculated following ohms law and power calculated according to:

179 $$P = V^2/R$$

180 Where,

181 V: is voltage across the resistance (in Volts)

182 R: external resistance (in Ohms)

183 All electrical data was related to the projected anodic area, which was considered to be
184 the base of the electrode (7.5 cm^2) in order to express power production per wetland
185 surface.

The maximum attainable voltage in a MFC (E_{emf}) is:

$$E_{emf} = E_{cat} - E_{an}$$

Where,

E_{cell}: cell voltage (in volts)

E_{cat}: is the redox at the cathode (in volts)

E_{an}: is the redox at the anode (in volts)

However, in a bioelectroquemical system cell performance is always affected by a number of losses that reduces the maximum attainable voltage (E_{emf}) to a cell voltage (E_{cell}) (Logan et al., 2006, Clauwaert et al., 2008). In the present work MFC efficiency was calculated as follows:

$$V_{eff} = \frac{Ecell}{E_{emf}} \cdot 100$$

It is important to note that average cell efficiency was calculated taking only into consideration E_{emf} values higher than 100 mV.

2.7 Microbial community assessment

2.7.1 DNA extraction

Wastewater samples from settler and HUSB were filtered in triplicate (5 mL each replicate) by means of Swinnex® Filter Holders (Millipore) with membrane filters of cellulose acetate (Whatman® 0.22 µm pore diameter). Filtrates were kept frozen at -20ºC until DNA extraction. Total DNA was extracted from influent wastewater filtrates, graphite material and gravel samples from both settler and HUSB lines. A bead beating DNA extraction was performed in triplicate by means of PowerSoil® DNA Isolation Kit (MoBio Laboratories, Solano Beach, CA, USA), following manufacturer's instructions.

2.7.2 Quantitative PCR assay

The ratios between eubacterial and methanogenic archaeal population were determined by quantifying the *16S* ribosomal *RNA* gene (*16S rRNA*) and the gene encoding of alpha

subunit of methyl-coenzyme M reductase (*mcrA*). Gene copy numbers of *16S rRNA* and *mcrA* fragments were quantified in triplicate with the quantitative real time PCR (qPCR) as elsewhere described (Sotres et al., in press). Standard curves were performed with known concentrations of the following reference cloned genes: *16S rRNA* gene from *Desulfovibrio vulgari*s subsp. *vulgaris* ATCC 29579, inserted in a TOPO TA vector (Invitrogen, Belgium); and a *mcrA* gene fragment obtained from *Methanosarcina barkeri* DSM 800 cloned a TOPO TA vector as well. The qPCR efficiencies of amplification were 92,2% and 90.4%, while the Pearson Correlation Coefficients (R^2) of the standard curves were between 0.999 and 0.971, and the slopes were between -3,524 and -3,575 for *16S rRNA* and *mcrA* gene, respectively.

All results were processed by MxPro™ QPCR Software (Stratagene, La Jolla, CA).

2.7.3 454-Pyrotag sequencing of total eubacterial and archaeal microbial populations

Massive bar-coded *16S rRNA* gene libraries targeting eubacterial region V1-V3 *16S rRNA* and archaeal region V3-V4 were sequenced utilizing 454 FLX Titanium equipment (Roche Diagnostics, Branford, CT, USA). In summary, diluted DNA extracts (1:10) were used as a template for PCR. Each DNA (two independent total DNA extract per sample) was amplified separately with both *16S rRNA* eubacteria and archaea set of primers containing unique multiplex identifier (MID) tags recommended by Roche Diagnostics (Roche Diagnostics, 2009). For eubacteria libraries the primer set were 27F (5'-AGRGTTTGATCMTGGCTCAG–3') and 519R (5'-GTNTTACNGCGGCKGCTG-3'), while archaeal set of primers were 349F (5'-GYGCASCAGKCGMGAAW-3') and 806R (5'–GGACTACVSGGGTATCTAAT-3'). The PCR conditions, subsequent purification and 454-pyrosequencing steps were performed as elsewhere described (Lladó et al., 2015). DNAs were sequenced utilizing Roche 454 FLX titanium instruments following manufacturer's guidelines.

Downstream 454-Pyrosequencing data analysis was carried out by using QIIME software version 1.8.0 (Caporaso et al., 2010a) following a trimming protocol and grouping into Operational Taxonomic Units (OTUs) as previously described (Lladó et al., 2015). OTUs were taxonomically classified using BLASTn against GreenGenes database and compiled into each taxonomic level (DeSantis, Hugenholtz et al. 2006).

Data from pyrosequencing datasets was submitted to the Sequence Read Archive (SRA) of the National Center for Biotechnology Information (NCBI) under the study accession number SRP042796.

2.8 Assessment of cathode limiting conditions

Results from the main experiment suggested that MFC performance was limited by the cathode surface applied. In order to confirm this hypothesis a short experiment was conducted at the end of the study period. The experiment consisted of increasing the surface of cathode up to five times than that of the anode for two of the MFC implemented in the HUSB line. More precisely, the cathode to anode surface ratios tested were that of 1:1, 1:5, 1:4, 1:3, 1:2 and again 1:1. E_{cell} was recorded by means of a datalogger (Datataker DT50 series 3) which collected a value of voltage across the external resistance every 15 minutes. E_{cell} was measured for three days at each cathode to anode surface ratio tested.

2.9 Statistical analyses

Differences among experimental conditions for any of the considered parameters (physico-chemical parameters, redox conditions and cell voltage) were determined by carrying out ANOVA tests, T-tests and Wilcoxon tests depending on the type of dataset being compared. Data normality and homogeneity of variances were determined by performing the Kolmogorov-Smirnoff and Levenne tests, respectively. Differences among experimental conditions were considered significant at p values bellow 0.05. All statistical analyses were performed using the software package R 3.0.2, with the exception of statistical multivariate analyses (covariance- based Principal Component Analyses PCA) of pyrosequencing data which was analyzed by means XLSTAT 2014 software (Addinsoft, Paris, France).

3 Results and discussion

3.1 Treatment performance

No differences were found between experimental lines for ammonia, nitrate, nitrite, sulphate and orthophosphate. Ammonia removal was 60%, regardless the experimental line considered (Table 1). Ammonia removal efficiency in HSSF CW usually ranges

from 40% to 55% (García et al. 2010). Higher ammonia removal rates here reported could be attributed to high evapotranspiration rates typical from small planted units (Pedescoll et al. 2013, Tanner 2001). Accordingly, water level variations impose higher redox conditions in wetlands which, in turn, may favour nitrification (García et al. 2003, García et al. 2010). In terms of organic matter, it was higher at the effluent of the HUSB reactor yet significant differences were only detected for the total COD. Hence, better removal rates for the settler line can be attributed to a lower organic loading rate when compared to the HUSB line. This result was already expected since the aim of the anaerobic reactor was to increase the total amount of biodegradable substrate supplied to the wetlands (Álvarez et al. 2008, Ligero et al. 2001). Moreover, samples extracted from the central part of the wetlands indicated that BOD_5, soluble and total COD in the vicinity of the MFC were significantly higher for the HUSB line when compared to the settler line. This result suggested that higher concentrations of substrate were available for the HUSB_MFCs which, in turn, could lead to a better performance of the cells (Cheng and Logan, 2011, Liu et al., 2004).

Furthermore, pH was mostly constant along the experiment and close to 7.5, regardless the type of primary treatment applied. Water temperature was, in average, 17.9 ± 5.2 ºC, with minimum values in February (6 ºC) and maximum values in July (28 ºC). Moreover, water temperature followed a daily cycle with temperature variations of about 2 ºC between day and night without significant differences among treatment lines.

Conductivity was significantly higher for the HUSB line when compared to the settler line. More precisely, conductivity was, in average, 2.69 ± 1.62 mS/cm and 3.37 ± 1.85 mS/cm to the settler and the HUSB line, respectively. Higher concentration of salts has been previously related to higher MFC performances (Cheng and Logan, 2011). This result suggested that cell performance could be higher for the HUSB line when compared to the settler line.

3.2 Redox and voltage pattern

Redox for both wetlands followed a very similar and conservative pattern. Redox potential at the anode was very constant and averaged -219 ± 29 mV (n= 1430) and -220 ± 46 mV (n=1177) for the HUSB and settler lines, respectively, without significant

differences among treatment lines. Redox potential at the cathode described a very constant day-night pattern, especially pronounced for the HUSB line (Figure 3). Accordingly, during nightly hours the redox potential at 5 cm depth was almost as reduced as that of 15 cm depth and, therefore, the redox gradient was almost zero. However, during sunlight hours the redox potential increased to a notable extent reaching maximum values between 200 and 300 mV, regardless the experimental line considered. Overall, and as has been previously described (Corbella et al., 2014), redox gradient between the anode and the cathode ranged between 400 and 500 mV, regardless the experimental line considered and, thus, no significant differences were recorded among experimental conditions.

Concerning cell voltage, MFC replicates performed similarly for both lines (Figure 4). Furthermore, it is widely accepted that cell electromotive force (E_{emf}) equals the difference between the cathode and the anode potential (redox gradient) minus the losses of the system (namely overpotentials and ohmic losses) (Logan et al., 2006). As expected, voltage recorded followed the same daily pattern than the redox gradient (Figure 4), showing picks during sunlight hours and being close to zero during nightly hours. Although there was a notable variability on the picks, cell voltage started to rise roughly between 11:00 and 15:00h and decreased between 18:00 and 23:00h.

During the first period, maximum daily cell voltage averaged 61 ± 29 mV and 50 ± 27 mV for the HUSB and the settler line, respectively. Although the HUSB line achieved a higher maximum cell voltage (136 mV when compared to 103 mV for the settler line), daily average cell voltage, yet higher for the HUSB line, was not significantly different among treatment lines. During the second period, HUSB_MFCs achieved a maximum cell voltage of 164 mV.

3.3 Effect of evapotranspiration on daily and seasonal cell performance

As it has been pointed out in the previous section, daily oscillations were observed all through the study period either in terms of redox (Figure 3) or cell voltage (Figure 4). Similar patterns have been reported in current literature for MFCs implemented in planted environments such as rice paddy fields (Kaku et al., 2008; De Schamphelaire et al., 2008) or, more recently, in constructed wetlands (Villaseñor et al., 2013). So far, an increase in the electrical output during sunlight hours is attributed to a higher

photosynthetic activity of plants that increases the total amount of substrate available (root exudates) for energy production (Strik et al., 2008; Kaku et al., 2008; De Schamphelaire et al., 2008). However, water losses caused by evapotranspiration in planted systems have been also described to influence MFC performance (Strik et al., 2008). Although water level inside the wetlands was set to be 30 cm, significant water level variations from the design value were observed all along the study period. More precisely, water level within the wetlands decreased from the design level in 3.1 ± 0.9 cm (in May where plants started to grow) to 6.1 ± 1.8 cm (in July where plants were already grown) (Figure 5). Moreover, intense water level variation, especially from May until the end of the study period, left the cathode of the MFC exposed to the atmosphere during the central hours of the day. When cathode was air-exposed, oxygen availability increased and favoured the current generation due to an increase of the cell voltage. Our results are in accordance with current literature since it is generally accepted that MFC performance is related to oxygen availability at the cathode (Fan et al., 2008; Oh et al., 2004).

Furthermore, our results suggested not only that cell voltage was influenced by water level variation on a daily basis, but also in terms of seasonal variations (Figure 6a and 6b). To this regard, from February until middle May, where temperature was that of 12.4 ± 4.4 ºC and plants were not yet developed, no significant power and current were recorded. From middle may until the end of July, when temperature rose up to 21.1 ± 5.1 ºC and plants were already developed, both current and power density started to increase, reaching maximum values during the first period (both HUSB and settler lines under operation) of 181 mA/m^2 and 25 mW/m^2 and 138 mA/m^2 and 14 mW/m^2 for the HUSB_MFCs and the SET_MFCs, respectively. During the second period (only the HUSB line) microbial fuel cells achieved the maximum power and current densities recorded for the whole study period (219 mA/m^2 and 36 mW/m^2). Average values for the first period were 82 ± 38 mA/m^2 and 6 ± 5 mW/m^2 and 66±37 mA/m^2 and 4 ± 4 mW/m^2 to the HUSB_MFCs and the SET_MFCs, respectively. Daily power production values (data not shown) followed also the same pattern than the current and power density, reaching maximum values during the first period of about 259 $mWh.m^{-2}.day^{-1}$ and 158 $mWh.m^{-2}.day^{-1}$ for the HUSB line and the settler line, respectively.

372 Regarding cell efficiency in the first period, voltage measured (E_{cell}) compared to the
373 maximum attainable (E_{emf}) was, in average, 13 ± 12% and 7 ± 5% to the HUSB and the
374 settler line, respectively. Therefore, results suggested that MFC were highly limited.
375
376 Power and current densities described by Villaseñor et al. (2013) and Yadav et al.
377 (2012) for MFC implemented in constructed wetlands are 43 mW/m^2 and of 16 mW/m^2
378 and 37 mA/m^2 and 70 mA/m^2, respectively. Therefore, our results are in the range of
379 that previously reported in literature, though this is the first time that, to the knowledge
380 of the authors, MFC are implemented in pilot-scale wetlands treating real domestic
381 wastewater, where the availability of easy biodegradable substrates is of lesser extent
382 when compared to synthetic wastewater. Overall, despite the HUSB line showed higher
383 maximum power production when compared to the settler line, no significant
384 differences were recorded among treatment lines. It is important to point out that
385 authors believe that one of the reasons behind the lack of significant differences among
386 treatment lines concerning the average cell voltage recorded was the high oxygen
387 limitation at the cathode. Indeed, the experiment on the assessment of cathode limitation
388 conditions performed at the end of the study period confirmed that MFC operated
389 during the whole period of study were probably subjected to a cathode limitation
390 surface (Figure 7). From Figure 7 it is clear that in order to avoid any cathode limiting
391 condition the surface of cathode shall be around four times higher than that of the
392 anode.

393 *3.4 Effect of primary treatment on bacterial populations in MFC-implemented CW*

394 Microbial community assessment was conducted on gravel, electrodes (graphite
395 material from open and closed circuit MFC) and from primary treated wastewater from
396 both the settler and HUSB reactor. Samples were taken from early June 2014. Total
397 eubacteria and archaea populations were determined by qPCR and *16S rRNA* gene
398 based 454 pyrotag sequencing approaches.

399 *3.4.1 Total eubacteria and methanogenic populations abundance*

400 Total microbial populations ranged from $2 \cdot 10^8$ to $6 \cdot 10^7$ *16S rRNA* gene copies $\cdot$ mL^{-1},
401 with methanogens accounting for 0.10-0.13% of total community in both the settler and
402 HUSB-treated wastewater. Total eubacteria (*16S rRNA* gene) and methanogenic archaea

in the effluent of the HUSB reactor were significantly lower ($P<0.05$) than that of the effluent of the settler (See supplementary material Figure S1; Table S1). Total eubacterial population recorded for both gravel and electrodes were not significantly different among experimental lines and ranged from $1 \cdot 10^8$ to $3 \cdot 10^8$ *16S rRNA* gene copies $\cdot g^{-1}$. Methanogenic population ranged from $0.6 \cdot 10^6$ *mcrA* gene copies g^{-1} to $1.2 \cdot 10^6$ *mcrA* gene copies g^{-1} (accounting for 0.22 to 0.49 % of total microbial populations) in graphite samples from active circuits of the settler and HUSB line, respectively. Furthermore, methanogenic populations were significantly higher ($P<0.05$) in the anode material of MFC operated at closed circuit (active circuit) when compared to gravel, regardless the primary treatment applied. However, only in case of the MFC within the settler line the methanogenic population were significantly different between active and inactive MFC.

3.4.2 16S rRNA gene-based 454 pyrotag sequencing of total eubacteria and archaea

Taking into account the slightly differences recorded regarding total eubacteria and methanogenic archaea abundance, a *16S rRNA* gene-based 454 pyrotag sequencing was carried out to gain insight on microbial community structure of total eubacteria and archaeal populations.

In the present study 16 samples for eubacteria and 14 for archaea were assessed. A total number of 136,925 and 72,233 sequences were obtained for eubacteria and archaea, respectively. After sequence processing, a total high-quality reads of 107,747 and 12,519 were retained for eubacteria and archaea, respectively. The average clean reads for eubacteria per sample were 5,794-8,304 for treated wastewater; 6,652-10,330 for the Settler line samples (gravel and graphite) and 5,020-6,667 reads for the HUSB line samples (gravel and graphite). The coverage (%) ranged from 95.9% to 98.9% for eubacteria and 94.6 to 99.9% for archaea (See supplementary material Table S2). However, the average cleaned reads taxonomically assigned as archaea per sample were from five to ten fold lower than those achieved for eubacteria (See supplementary material Table S2). The number of OTUs (97% of similarity) for eubacteria ranged from 352 to 434 in wastewater samples, and from 436 to 775 for graphite and gravel samples. The number of high quality reads for eubacteria were not significantly different among experimental lines, regardless the type of sample considered (primary treated wastewater, gravel, and graphite samples). However, significantly higher diversity was

435 encountered for the HUSB line samples when compared to the settler line based on
436 certain diversity estimators such as OTU numbers (640-775), Chao-1 (837-987),
437 Shannon-Wienner (5.0-5.5), and even a higher evenness index (0.23-0.38) (See
438 supplementary material Figure S2 and Table S2).

439 Global diversity results clearly showed the existence of a population shift in MFC
440 implemented in constructed wetlands, specially driven by HUSB pretreated wastewater.
441 The diversity encountered in our 454 *16S rRNA* gene pyrotag libraries in MFC coupled
442 CWs (Shannon index (*H*) in the range of 4.36 to 5.5) was significantly higher than that
443 described elsewhere in constructed wetlands treating domestic wastewater and swine
444 wastewater using the DGGE technique (*H*: 1.1-4 (Calheiros et al., 2009); H: 0.71-1.07
445 (Dong and Reddy, 2010); tRFLP (*H*: 2.9-3.1) or those using clone libraries (H: 2-3.8) in
446 CW treating industrial wastewater polluted with arsenic and zinc (Arroyo et al., 2013).

447 Biodiversity of eubacteria (by class) and archaea (by family) in terms of relative
448 incidence for the main taxonomic groups are shown in Figure 8a and b (and also in
449 Table S3). Settled wastewater showed a high predominance of beta-proteobacteria
450 (average 29%) and Flavobacteria (average 48%) (Figure 8a; Supplementary material
451 Table S3). Anaerobically pre-treated wastewater showed a predominance of beta and
452 gamma-proteobacteria (average 46% and 32%, respectively) and, to a lesser extent,
453 flavobacteria (6%) and clostridia (7%).

454 Samples analyzed for eubacteria from the wetland fed with the settler effluent
455 (including gravel and graphite at open and close circuit MFC) presented no significant
456 differences concerning the dominance of groups at class level (Fig. 8a and b; Table S3).
457 Among eubacteria dominant classes were that of alfa-proteobacteria (around 20-32%)
458 and Flavobacteria (around 16-30%).

459 Samples analyzed for eubacteria from within the wetland fed with the HUSB effluent
460 (including gravel and graphite at open and close circuit MFC) also showed no
461 significant differences concerning the dominance of groups at class level (Fig. 8a and b;
462 Table S3). Among eubacteria dominant classes were that of Alphaproteobacteria (up to
463 17%), Deltaproteobacteria (up to 30%); clostridia (up to 18%); bacterioidia (up to ca.
464 8%); synergistia (up to 9%) and anaerolineae (up to 6%).

Diversity of eubacteria was significantly higher, encompassing important phylogenetic and quantitative changes, when the HUSB line was compared to the Settler line, regardless the type of sample considered (Fig. 8a; Table S3). More precisely, for gravel and graphite samples of the HUSB line predominant groups were that of clostridia, delta-proteobacteria, Bacteroidia, Synergistia, alfa-proteobacteria and Anaerolineae (Figure 8; Table S3 and S4). Accordingly, the fundamental difference in microbial community structure promoted by the two types of primary treatment here considered was the high enrichment in Bacteroidia (OTUs 1 and 2) and delta-proteobacteria class in the gravel and graphite samples of the HUSB line (OTU 4) when compared to gravel and graphite samples of the settler line.

Regarding delta-proteobacteria class it is remarkable the relative predominance of the Geobacteraceae family in gravel and graphite samples of the HUSB line (19% and 5% of relative abundance for the graphite of active MFC and gravel samples, respectively). Within the Geobacteraceae family it is of special interest the high relative abundance of one OTU belonging to *Geobacter* in active MFC of the HUSB line (from 13 to 16%). In the case of gravel and graphite samples from the settler line, Geobacteraceae were not only less favored (below 2%), but even the detected Geobacteraceae OTUs were different from that of the OTUs found in samples from the HUSB line (Table S5).

Regarding archaeal population, it is noteworthy the high relative prevalence of Methanosaetaceae family at the effluent of both types of primary treatments (55% and 81% for the settler and HUSB reactor, respectively). Furthermore, there was a shift in methanogenic archaea that consisted in a high decrease of Methanosaetaceae encompassed by an enrichment of Methanomicrobiaceae/Thermoplasmata (OTU2) as it is assigned by Greengenes/RDP Bayesian Classifier in HUSB line. In addition, a non methanogenic phylum (Chrenarchaeaota) was highly predominant in gravel and graphite samples from both experimental lines. (Chrenarchaeota, assigned as Fervidicoccaceae/Thermoprotei by Greengenes/RDP Bayesian Classifier) (Wang et al., 2007) (37-53% and 23-39% to the settler and HUSB lines, respectively).

Multivariate statistical analyses were conducted by means of covariate-principal component analyses (PCA) (Figure 9a,b, and Figure S3-S4) and correspondence analyses (CA) with similar results. PCA and CA analysis revealed the existence of three main separate groups of samples encompassing different microbial communities

(primary treated wastewater samples, settler line and HUSB line) (Figure 9 a,b). Regarding eubacteria, the main OTUs with the higher component weight/contribution in wastewater were OTUs 8 and 673, closely similar to *Comamonas denitrificans* (beta-proteobacteria) and OTUs 10 and 224 belonging to well known fermentative *Acinetobacter* genus (gamma-protebacteria). Regarding the settler line, OTUs belonging to *Cloacibacterium* (Bacteroidetes, OTU 1), *Phenylobacterium* (alpha-proteobacteria, OTU 3) and *Sphingopixis* (alpha-proteobacteria, OTU 7) were the main OTUs to define the group. For the HUSB line it is worth mentioning the presence of two main distinctive OTUs on PCA/CA biplot (Figure 9 a,b and Fig S3-4), OTU 2 belonging to *Rhodobacter/Bacteroidetes* (assigned by Greengenes/RDP Bayesian classifier databases, and OTU 4, closely similar in sequence (99.7%) to an environmental *Geobacter* (delta-proteobacteria) and to *Geobacter lovleyi* Geo 7.1A (97.16%). OTU 4 was not detected neither in primary treated wastewater nor in the settler line, and was clearly more enriched in anode under closed (active) circuit (13-16%) for the HUSB line than in gravel (3%), and almost absent (0.6-1.5%) in opened (inactive) circuit (Table S3). Taking into account that MFC within the HUSB line tended to show higher current and power densities when compared to the settler line, OTU 4 related with *Geobacter* might be a good candidate as a key player for exoelectrogenic and current production in this system. Coincidently, a *Geobacter* enrichment was also reported in constructed wetlands treating 1,2-dichloroethene-contaminated groundwater (Imfeld et al., 2010), and recently in the anode of lab-scale MFC coupled to a constructed wetland system for decolorization of azo dyes (Fang et al., 2013). However, contrarily to Fang et al. (2013), in the present study methanogenic archaea belonging to *Methanosaeta* has been just slightly enriched in the anode material of both experimental lines (Table S5). Current research is revealing the occurrence of exoelectrogenic activity in *Methanosarcina* and *Methanosaeta* sharing electrons with a concomitant *Geobacter*, (Rotaru et al.,2014 a, b) promoting potential electron current production in MFCs and complex microbial communities such as those harboured in natural environments.

4 Conclusions

The settler line slightly outperformed the HUSB line in terms of treatment efficiency, though only in terms of total COD differences were significantly different.

528 Maximum current and power densities recorded with microbial fuel cells implemented
529 in constructed wetlands for the treatment of real domestic wastewater was that of 219
530 mA/m^2 and 36 mW/m^2.

531 Microbial fuel cells implemented in constructed wetlands receiving the effluent of an
532 anaerobic reactor showed higher current and power densities than microbial fuel cells
533 implemented in the wetlands receiving primary settled wastewater. However,
534 differences among treatment lines were not significantly different. The lack of
535 significant differences was probably due to a cathode surface limitation.

536 Redox gradient between electrodes and cell voltage followed a very conservative
537 pattern along the day with higher output cell voltage values during daylight hours. The
538 main parameter controlling the cell voltage was water level variation within the
539 wetlands that resulted from intense evapotranspiration and exposed the cathode to air.

540 The type of primary treatment implemented had a significant impact on the diversity
541 and relative abundance of bacteria communities colonizing MFC. It is worth noticing
542 the high predominance (13-16% of relative abundance) of one OTU belonging to
543 *Geobacter* on active MFC of the HUSB line that was absent for the settler line MFC.

544 ## 5 Acknowledgements

545 This study was funded by the Spanish Ministry of Science and Innovation (MICINN)
546 (project CTM2010-17750).

547 ## 6 References

548 Álvarez, J. a., Ruíz, I., Soto, M, 2008. Anaerobic digesters as a pretreatment for
549 constructed wetlands. Ecological Engineering 33(1), 54–67.

550 APHA-AWWA-WEF, 2005. Standard Methods for the Examination of Water and
551 Wastewater. 21st ed. American Public Health Association, Washington, DC.

552 Arroyo, P., Ansola, G., Miera. L.E., Effects of substrate, vegetation and flow on arsenic
553 and zinc removal efficiency and microbial diversity in constructed wetlands.
554 Ecological Engineering 51, 95-103.

555 Baptista, J. D. C., Donnelly, T., Rayne, D., Davenport, R. J., 2003. Microbial
556 mechanisms of carbon removal in subsurface flow wetlands. Water Science and
557 Technology : A Journal of the International Association on Water Pollution
558 Research 48(5), 127–34.

559 Borole, A. P.; Reguera, G.; Ringeisen, B.; Wang, Z.-W.; Feng, Y.; Kim, B. H., 2011.
560 Electroactive biofilms: Current status and future research needs. Energy Environ.
561 Sci. 4, 4813-4834

562 Calheiros, C. S., Duque, A. F., Moura, A., Henriques, I. S., Correia, A., Rangel, A. O.,
563 Castro, P. M., 2009. Changes in the bacterial community structure in two-stage
564 constructed wetlands with different plants for industrial wastewater treatment.
565 Bioresource technology, 100(13), 3228-3235.

566 Caporaso, J. G., J. Kuczynski, J. Stombaugh, K. Bittinger, F.D. Bushman, E.K.
567 Costello, N. Fierer, A. Gonzalez-Pena, J.K. Goodrich, J.I. Gordon, G.A. Huttley,
568 S.T. Kelley, D. Knights, J.E. Koenig, R.E. Ley, C.A. Lozupone, D. McDonald,
569 B.D. Muegge, M. Pirrung, J. Reeder, J.R. Sevinsky, P.J. Turnbaugh, W.A.
570 Walters, J. Widmann, T. Yatsunenko, J. Zaneveld, R. Knight, 2010a. QIIME
571 allows analysis of high-throughput community sequencing data. Nature Methods
572 7, 335-336.

573 Caporaso, J.G., K. Bittinger, F.D. Bushman, T.Z. DeSantis, G.L. Andersen, R. Knight,
574 2010b. PyNAST: A flexible tool for aligning sequences to a template alignment.
575 Bioinformatics 26, 266-267.

576 Cheng, S., Logan, B. E., 2011. Increasing power generation for scaling up single-
577 chamber air cathode microbial fuel cells. Bioresource Technology, 102(6), 4468–
578 73.

579 Chung K and Okabe S, 2009. Continuous power generation and microbial community
580 structure of the anode biofilms in a three-stage microbial fuel cell system. Applied
581 Microbiology and Biotechnology 83: 965-977.

582 Clauwaert, P., Aelterman, P., Pham, T. H., De Schamphelaire, L., Carballa, M., Rabaey,
583 K., Verstraete, W., 2008. Minimizing losses in bio-electrochemical systems: the
584 road to applications. Applied Microbiology and Biotechnology 79(6), 901–13.

585 Corbella, C., Garfí, M., Puigagut, J., 2014. Vertical redox profiles in treatment wetlands
586 as function of hydraulic regime and macrophytes presence: Surveying the optimal
587 scenario for microbial fuel cell implementation. Science of the Total
588 Environment, 470-471, 754–8.

589 DeSantis, T. Z., Hugenholtz, P., Larsen, N., Rojas, M., Brodie, E. L., Keller, K., …
590 Andersen, G. L., 2006. Greengenes, a chimera-checked 16S rRNA gene database
591 and workbench compatible with ARB. Applied and Environmental Microbiology,
592 72(7), 5069–72.

593 De Schamphelaire, L., Van den Bossche, L., Dang, H. S., Höfte, M., Boon, N., Rabaey,
594 K., Verstraete, W., 2008. Microbial fuel cells generating electricity from
595 rhizodeposits of rice plants. Environmental Science & Technology, 42(8), 3053–
596 8.

597 Dong, X., Reddy, G. B., 2010. Soil bacterial communities in constructed wetlands
598 treated with swine wastewater using PCR-DGGE technique. Bioresource
599 technology, 101(4), 1175-1182.

600 Dušek, J., Picek, T., Čížková, H., 2008. Redox potential dynamics in a horizontal
601 subsurface flow constructed wetland for wastewater treatment: Diel, seasonal and
602 spatial fluctuations. Ecological Engineering, 34(3), 223–232.

603 Du, Z., Li, H., Gu, T., 2007. A state of the art review on microbial fuel cells: A
604 promising technology for wastewater treatment and bioenergy. Biotechnology
605 Advances, 25(5), 464–82.

606 Fang, Z., Song, H.-L., Cang, N., Li, X.-N. 2013. Performance of microbial fuel cell
607 coupled constructed wetland system for decolorization of azo dye and
608 bioelectricity generation. Bioresource Technology, 144, 165–71.

609 Fan, Y., Sharbrough, E., & Liu, H., 2008. Quantification of the internal resistance
610 distribution of microbial fuel cells. Environmental Science & Technology, 42(21),
611 8101–7.

612 García, J., Ojeda, E., Sales, E., Chico, F., Píriz, T., Aguirre, P., Mujeriego, R., 2003.
613 Spatial variations of temperature, redox potential, and contaminants in horizontal
614 flow reed beds. Ecological Engineering, 21(2-3), 129–142.

615 García, J., Rousseau, D. P. L., Morató, J., Lesage, E., Matamoros, V., Bayona, J. M.,
616 2010. Contaminant Removal Processes in Subsurface-Flow Constructed
617 Wetlands: A Review. Critical Reviews in Environmental Science and
618 Technology, 40(7), 561–661.

619 Gonçalves, R. F., Charlier, A. C., Sammut, F., 1994. Primary fermentation of soluble
620 and particulate organic matter for wastewater treatment. Water Science and
621 Technology: A Journal of the International Association on Water Pollution
622 Research, 30(6), 53–62.

623 Imfeld, G., Aragonés, C. E., Fetzer, I., Mészáros, É., Zeiger, S., Nijenhuis, I., ...
624 Richnow, H. H., 2010. Characterization of microbial communities in the aqueous
625 phase of a constructed model wetland treating 1, 2-dichloroethene-contaminated
626 groundwater. FEMS microbiology ecology, 72(1), 74-88.

627 Kaku, N., Yonezawa, N., Kodama, Y., Watanabe, K., 2008. Plant/microbe cooperation
628 for electricity generation in a rice paddy field. Applied Microbiology and
629 Biotechnology, 79(1), 43–9.

630 Kiely P.D, Regan J.M, Logan B.E., 2011. The electric picnic: synergistic requirements
631 for exoelectrogenic microbial communities. Current Opinion in Biotechnology,
632 22:378-385.

633 Lefebvre, O., Uzabiaga, A., Chang, I. S., Kim, B.-H., Ng, H. Y., 2011. Microbial fuel
634 cells for energy self-sufficient domestic wastewater treatment-a review and
635 discussion from energetic consideration. Applied Microbiology and
636 Biotechnology, 89(2), 259–70.

637 Ligero, P., Vega, A., Soto, M., 2001. Pretreatment of urban wastewaters in a hydrolytic
638 upflow digester, 27(3), 399–404.

639 Liu, H., Ramnarayanan, R., Logan, B. E., 2004. Production of electricity during
640 wastewater treatment using a single chamber microbial fuel cell. Environmental
641 Science & Technology, 38(7), 2281–5.

642 Lladó, S., Covino, S., Solanas, A.M., Petruccioli, M., D'annibale, A. and Viñas M.,
643 2015. Pyrosequencing reveals the effect of mobilizing agents and lignocellulosic

substrate amendment on microbial community composition in a real industrial PAH-polluted soil. Journal of Hazardous Materials, 283, 35-43

Logan, B. E., Hamelers, B., Rozendal, R., Schröder, U., Keller, J., Freguia, S.Rabaey, K., 2006. Microbial fuel cells: methodology and technology. Environmental Science & Technology, 40(17), 5181–92.

Logan, B.E., 2009. Exoelectrogenic bacteria that power microbial fuel cells. Nature Reviews in Microbiology, 7, 375-381.

Min, B., Logan, B. E., 2004. Continuous electricity generation from domestic wastewater and organic substrates in a flat plate microbial fuel cell. Environmental Science & Technology, 38(21), 5809–14.

Nevin KP, Richter H, Covalla SF, Johnson JP, Woodard TL, Orloff AL, Jia H, Zhang M and Lovley DR., 2008. Power output and columbic efficiencies from biofilms of Geobacter sulfurreducens comparable to mixed community microbial fuel cells. Environ Microbiol 10: 2505-2514

Oh, S., Min, B., Logan, B. E., 2004. Cathode performance as a factor in electricity generation in microbial fuel cells. Environmental Science & Technology, 38(18), 4900–4.

Pedescoll, A., Corzo, A., Alvarez, E., García, J., Puigagut, J., 2011a. The effect of primary treatment and flow regime on clogging development in horizontal subsurface flow constructed wetlands: An experimental evaluation. Water Research, 45(12), 3579–89.

Pedescoll, A., Corzo, A., Álvarez, E., Puigagut, J., García, J., 2011b. Contaminant removal efficiency depending on primary treatment and operational strategy in horizontal subsurface flow treatment wetlands. Ecological Engineering, 37(2), 372–380.

Pedescoll, A., Sidrach-Cardona, R., Sánchez, J. C., Bécares, E., 2013. Evapotranspiration affecting redox conditions in horizontal constructed wetlands under Mediterranean climate: Influence of plant species. Ecological Engineering, 58, 335–343.

673 Rabaey K, Boon N, Siciliano S.D, Verhaege M and Verstraete W., 2004. Biofuel cells
674 select for microbial consortia that self-mediate electron transfer. Applied and
675 Environmental Microbiology 70:5373–5382.

676 Rabaey, K., & Verstraete, W., 2005. Microbial fuel cells: novel biotechnology for
677 energy generation. Trends in Biotechnology, 23(6), 291–8.

678 Rabaey, K., Rodríguez, J., Blackall, L. L., Keller, J., Gross, P., Batstone, D., Nealson,
679 K. H., 2007. Microbial ecology meets electrochemistry: electricity-driven and
680 driving communities. The ISME Journal, 1(1), 9–18.

681 Reimers, C. E., Tender, L. M., Fertig, S., Wang, W., 2001. Harvesting energy from the
682 marine sediment--water interface. Environmental Science & Technology, 35(1),
683 192–5.

684 Rezaei, F., Richard, T. L., Brennan, R. a, Logan, B. E., 2007. Substrate-enhanced
685 microbial fuel cells for improved remote power generation from sediment-based
686 systems. Environmental Science & Technology, 41(11), 4053–8.

687 Richter H, Mc Carthy K, Nevin KP, Johnson JP, Rotello VM and Lovley DR, 2008.
688 Electricity generation by Geobacter sulfurreducens attached to gold electrodes.
689 Langmuir 24: 4376-4379.

690 Ringeisen BR, Henderson E, Wu PK, Pietron J, Ray R, Little B, Biffinger JC and Jones-
691 Meehan JM, 2006. High power density from a miniature microbial fuel cell using
692 Shewanella oneidensis DSP10. Environmental Science & Technology 40: 2629-
693 2634.

694 Roche Diagnostics. 2009. Using multiple identifier (MID) adaptors for the GS FLX
695 titanium chemistry-extended MID set. Technical Bulletin: Genome Sequencer
696 FLX System.

697 Rotaru A, Shrestha P, Liu F, Shrestha M, Shrestha D, Embree M, Zengler K, Wardman
698 C, Nevin KP and Lovley DR, 2014a. A new model for electron flow during
699 anaerobic digestion: direct interspecies electron transfer to *Methanosaeta* for the
700 reduction of carbon dioxide to methane. Energy Environ Sci 7: 408-415.

Rotaru, A. E., Shrestha, P. M., Liu, F., Markovaite, B., Chen, S., Nevin, K., Lovley, D., 2014b. Direct interspecies electron transfer between Geobacter metallireducens and Methanosarcina barkeri. Applied and environmental microbiology, AEM-00895.

Sotres, A, Diaz-Marcos, J., Guivernau, M., Illa, J., Magrí, A., Prenfeta-Boldú, F.X., Bonmatí, A., Viñas, M., 2014. Microbial community dynamics in two-chambered microbial fuel cells: effect of different ion exchange membranes'. Journal of Chemical Technology and Biotechnology. In Press DOI 10.1002/jctb.4465.

Strik, D. P. B. T. B., Snel, J. F. H., Buisman, C. J. N., 2008. SHORT COMMUNICATION Green electricity production with living plants and bacteria in a fuel cell, (January), 870–876.

Tanner, C. C., 2001. Plants as ecosystem engineers in subsurface-flow treatment wetlands. Water Science and Technology□: A Journal of the International Association on Water Pollution Research, 44(11-12), 9–17.

Villaseñor, J., Capilla, P., Rodrigo, M. a, Cañizares, P., & Fernández, F. J., 2013. Operation of a horizontal subsurface flow constructed wetland--microbial fuel cell treating wastewater under different organic loading rates. Water Research, 47(17), 6731–8.

Wang, Q., Garrity, G.M., Tiedje, J.M., Cole, J.R., 2007. Naive Bayesian classifier for rapid assignment of rRNA sequences into the new bacterial taxonomy. Appl. Environ. Microbiol. 73, 5261–5267.

Xing, D., Cheng, S., Logan, B.E., Regan, J.M., 2010. Isolation of the exoelectrogenic denitrifying bacterium Comamonas denitrificans based on dilution to extinction. Applied Microbiology and Biotechnology, 85, 1575-1587

Yadav, A. K., Dash, P., Mohanty, A., Abbassi, R., Mishra, B. K., 2012. Performance assessment of innovative constructed wetland-microbial fuel cell for electricity production and dye removal. Ecological Engineering, 47, 126–131.

Zhao, Y., Collum, S., Phelan, M., Goodbody, T., Doherty, L., Hu, Y., 2013. Preliminary investigation of constructed wetland incorporating microbial fuel cell: Batch and continuous flow trials. Chemical Engineering Journal, 229, 364–370.

Table
Click here to download Table: Tables.docx

Table 1. Physical and chemical parameters measured. *Note*: average values are shown with standard deviation in brackets.

		HUSB				SETTLER			
		in	middle	out	% removal	in	middle	out	% removal
$DBO_{soluble}$ (n=7)	*(mg O_2 /L)*	137 (63)	71 (26)*	76 (63)	55	115 (53)	37 (14)*	42 (25)	54
COD_{total} (n=17)	*(mg O_2 /L)*	323 (33)*	137 (53)*	126 (60)*	61	235 (19)*	100 (46)*	69 (29)*	71
AMMONIA (n=16)	*(mg $NH4^+$-N/L)*	41 (7)	-	19 (19)	58	39 (8)	-	17 (17)	60
NITRATE (n=13)	*(mg NO_3-N/ L)*	< 1	-	< 1	-	< 1	-	< 1	-
NITRITE (n=13)	*mg NO_2-N/ L*	< 1	-	< 1	-	< 1	-	< 1	-
SULPHATE (n=13)	*(mg SO_4^{2-}/L)*	102 (27)	-	68 (53)	34	113 (37)	-	68 (71)	40
ORTHOPHOSPHATE (n=13)	*(mg P-PO_4^3 /L)*	9 (3)	-	10 (7)	-	7 (2)	-	5 (5)	-

* Significant differences among treatment lines.

Figures

Figure 1. Microbial fuel cells implemented within the wetland at the beginning of the experiment.

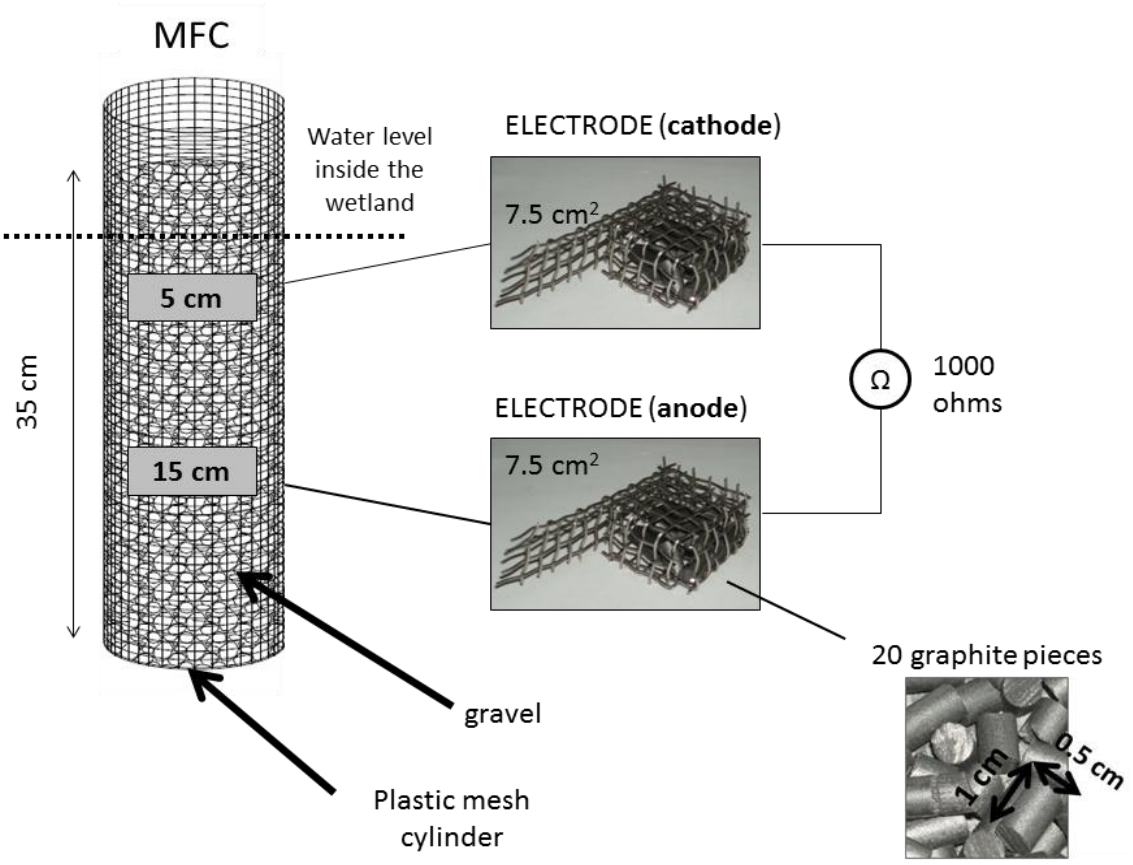

Figure 2. Outline of microbial fuel cells and electrodes.

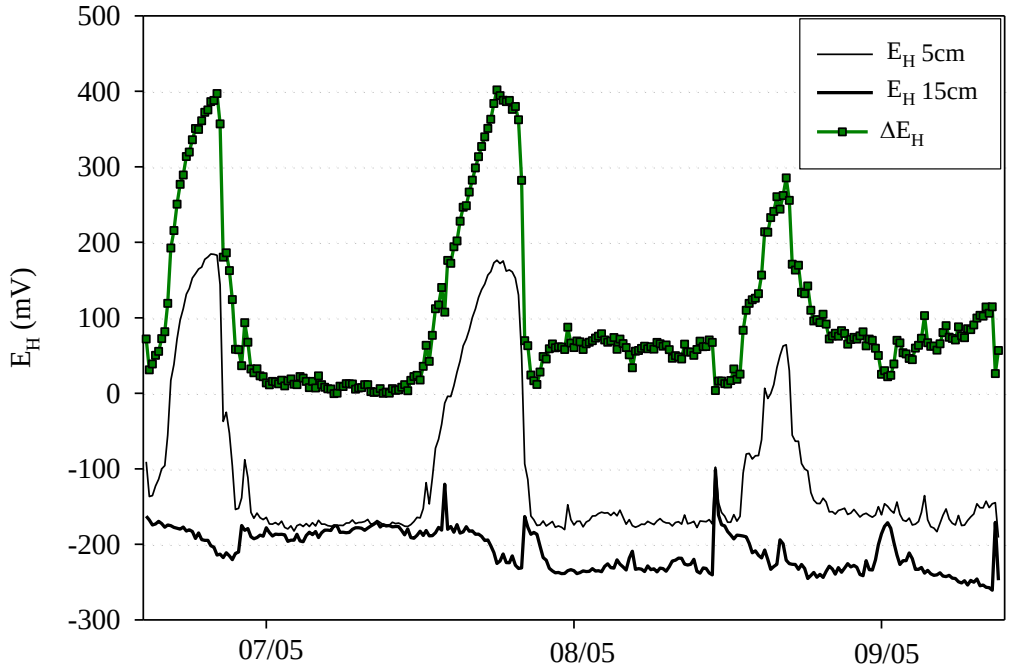

Figure 3. Representative redox daily pattern for the HUSB line.

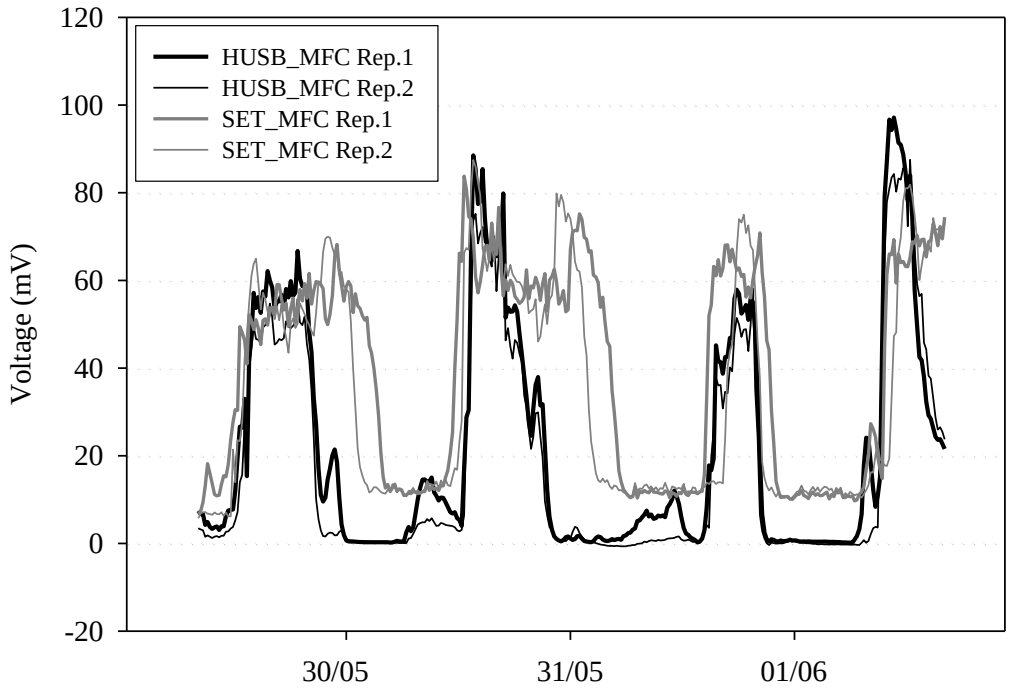

Figure 4. Representative voltage pattern recorded for microbial fuel cells implemented within the HUSB and the Settler line.

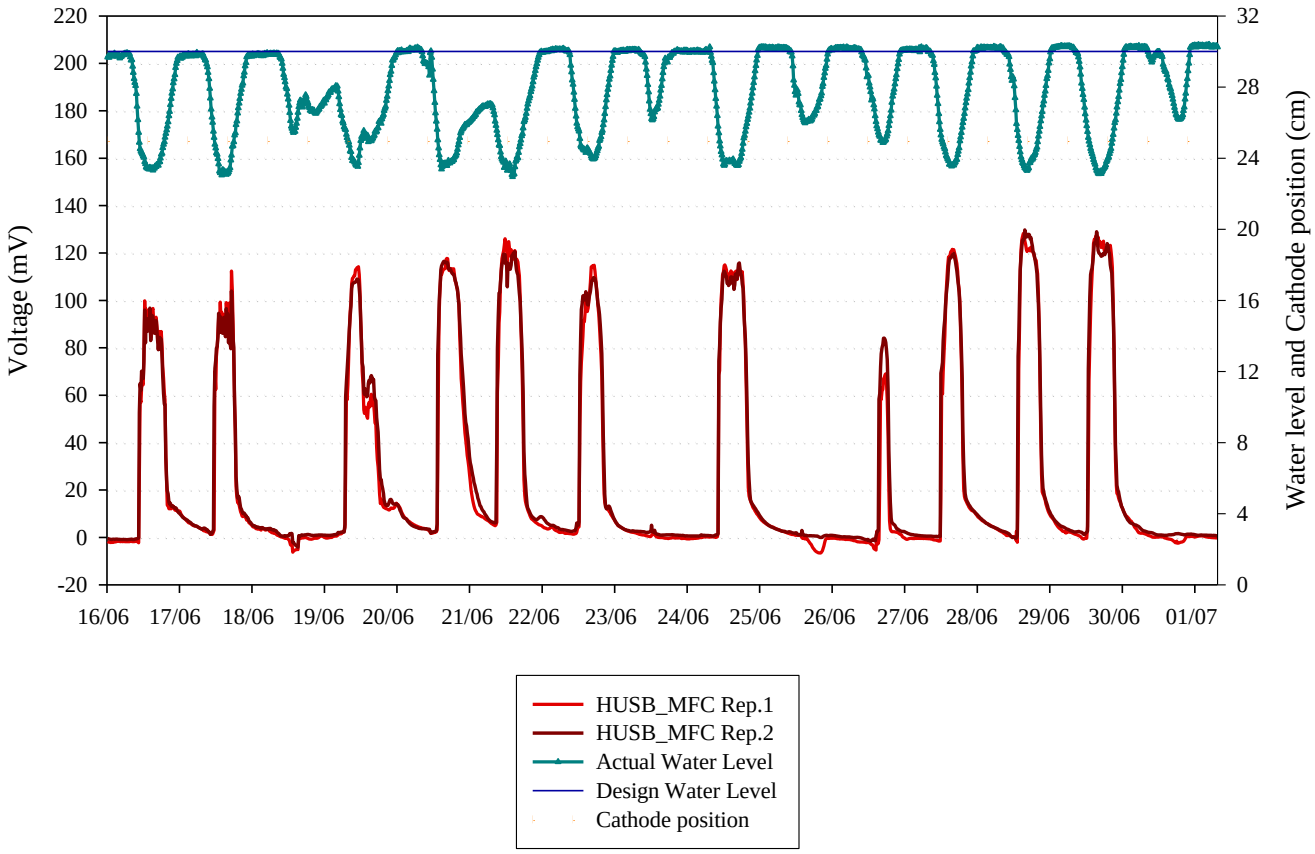

Figure 5. Representative cell voltage and water level variation for the HUSB line.

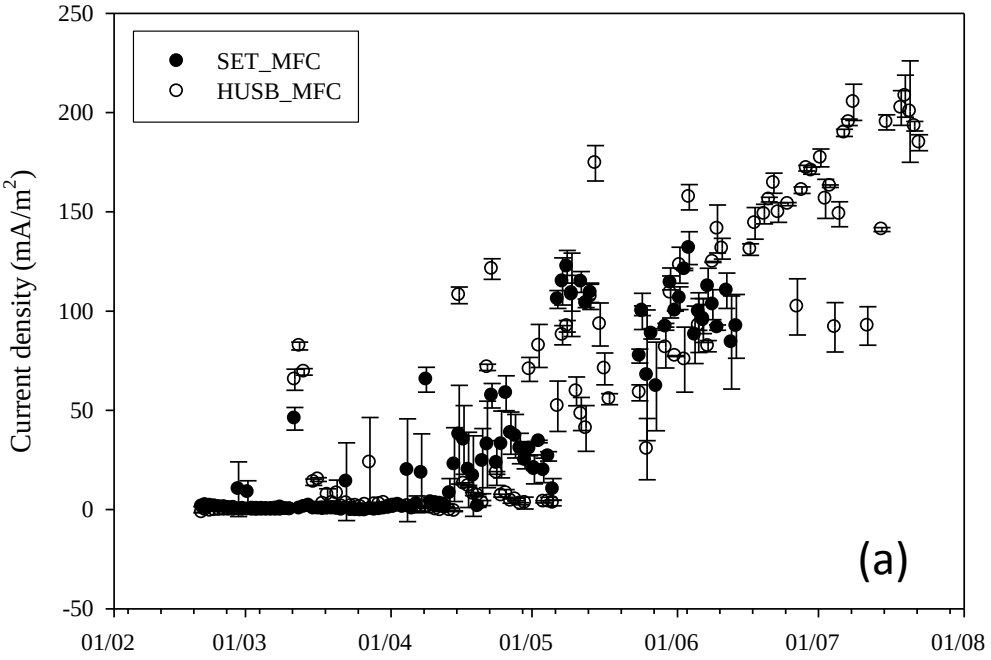

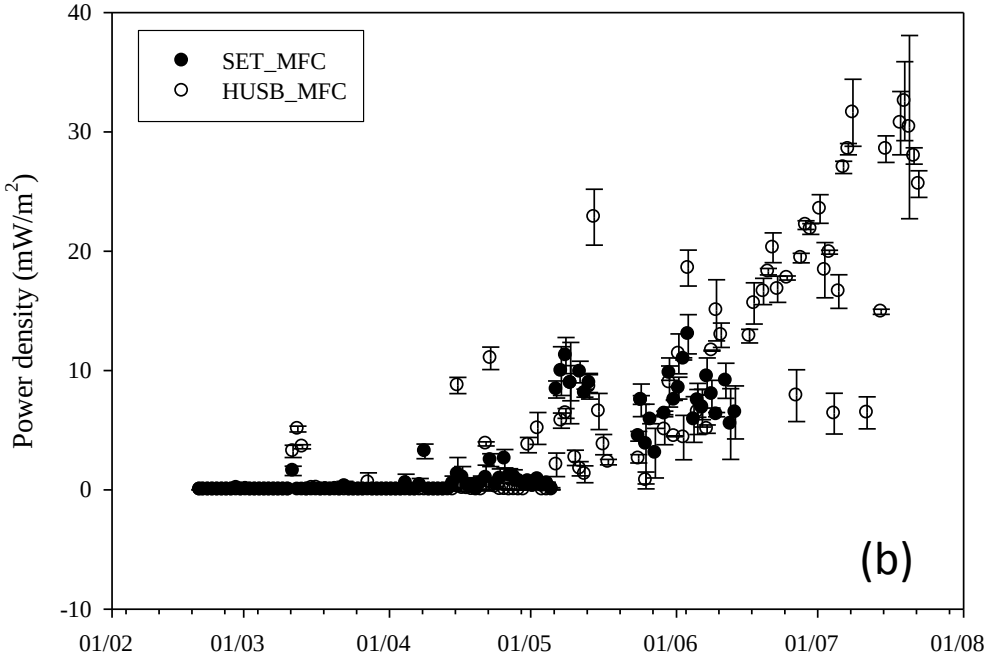

Figure 6. Daily maximum current (a) and power (b) density evolution along the experiment for the HUSB_MFCs and the SET_MFCs. Note that values from the settler line are only plotted until middle June since after then, only the HUSB line was left under operation.

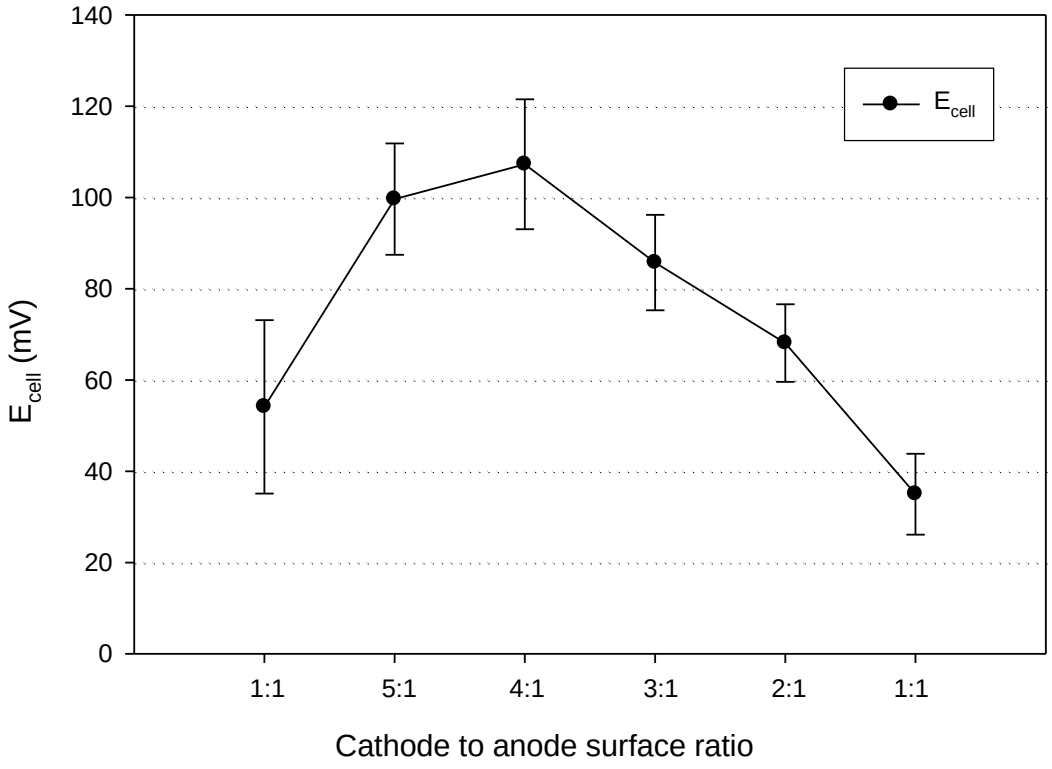

Figure 7. Influence of cathode to anode surface ratio on E_{cell}. *Note*: error bars are the standard deviation of two replicates; each dot represents a three-day average value of the E_{cell} recorded during sunlight hours.

A)

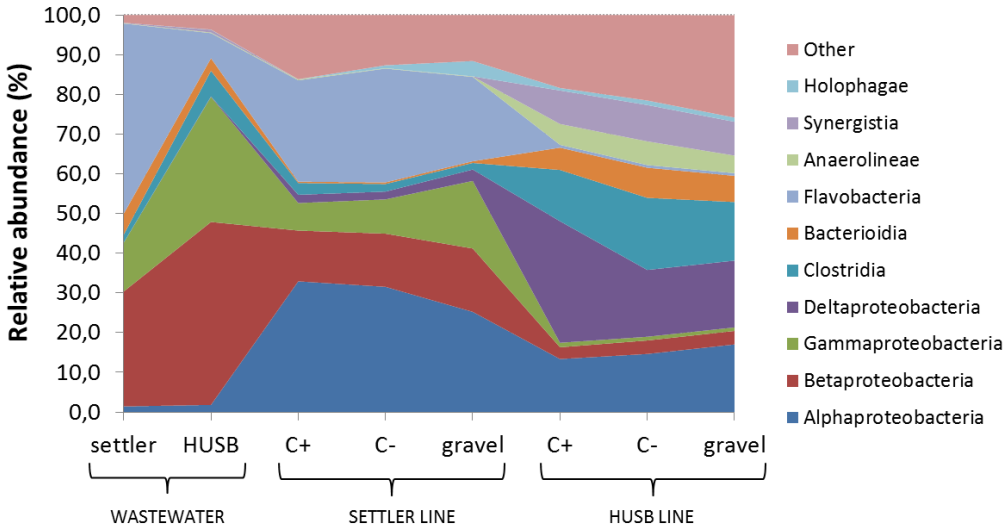

B)

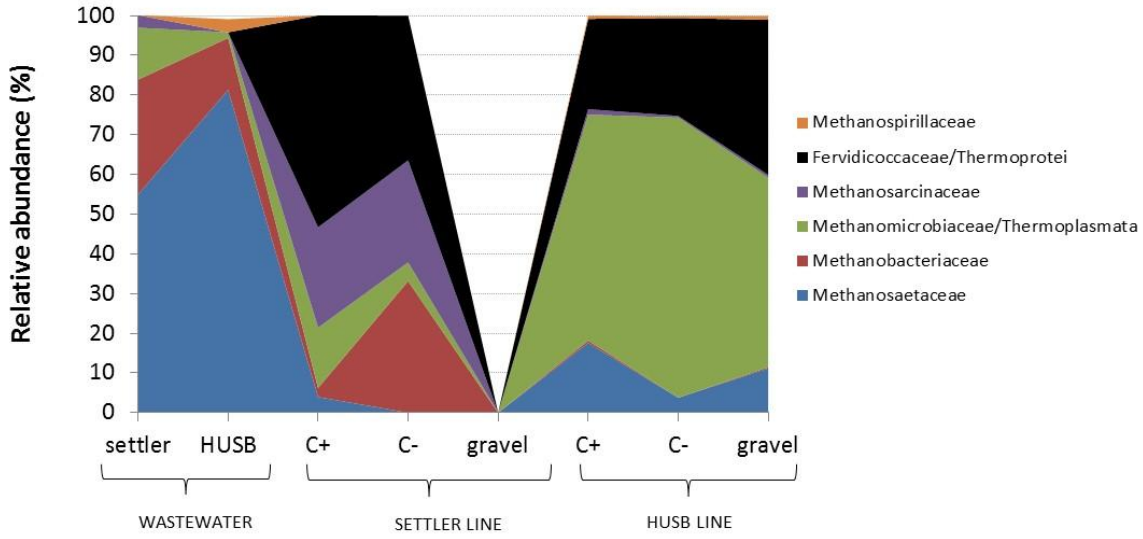

Figure. 8. Biodiversity of main representatives of eubacteria (sorted by class) (A) and archaea (sorted by family) (B) expressed as relative OTUs abundance (%).Thermoprotei class or Fervidicocacceae family in Chrenarchaeota phylum were assigned according RDP Classifier and greengenes respectively. Thermoplasmata class or Methanomicrobiaceae in Euryarchaeota phylum were assigned according RDP Classifier and greengenes respectively. *Note*: gravel samples from the settler line did not produce any DNA amplification and are not considered in Figure 7B.

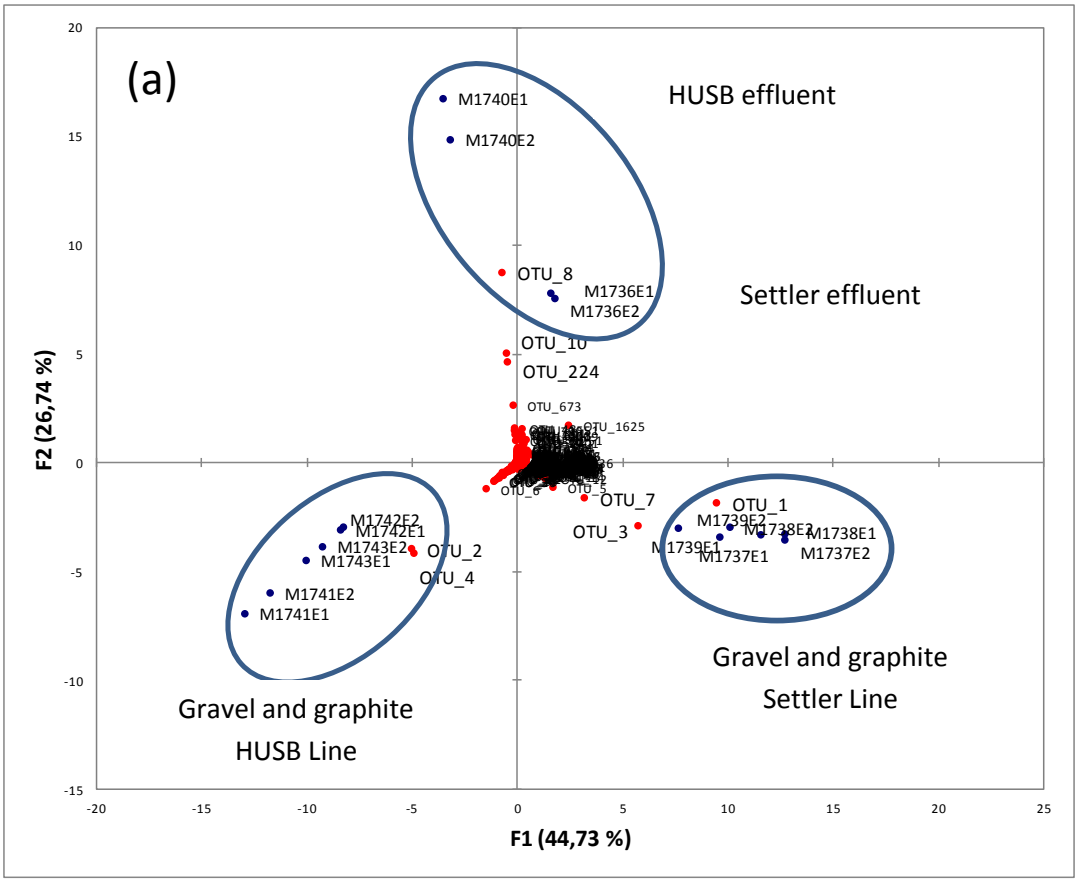
(a)
HUSB effluent
Settler effluent
Gravel and graphite
Settler Line
Gravel and graphite
HUSB Line
M1740E1
M1740E2
OTU_8
M1736E1
M1736E2
OTU_10
OTU_224
OTU_673
OTU_1625
OTU_7
OTU_3
OTU_1
M1739E2
M1738E2
M1738E1
M1739E1
M1737E1
M1737E2
M1742E2
M1742E1
M1743E2
M1743E1
OTU_2
OTU_4
M1741E2
M1741E1
F2 (26,74 %)
F1 (44,73 %)

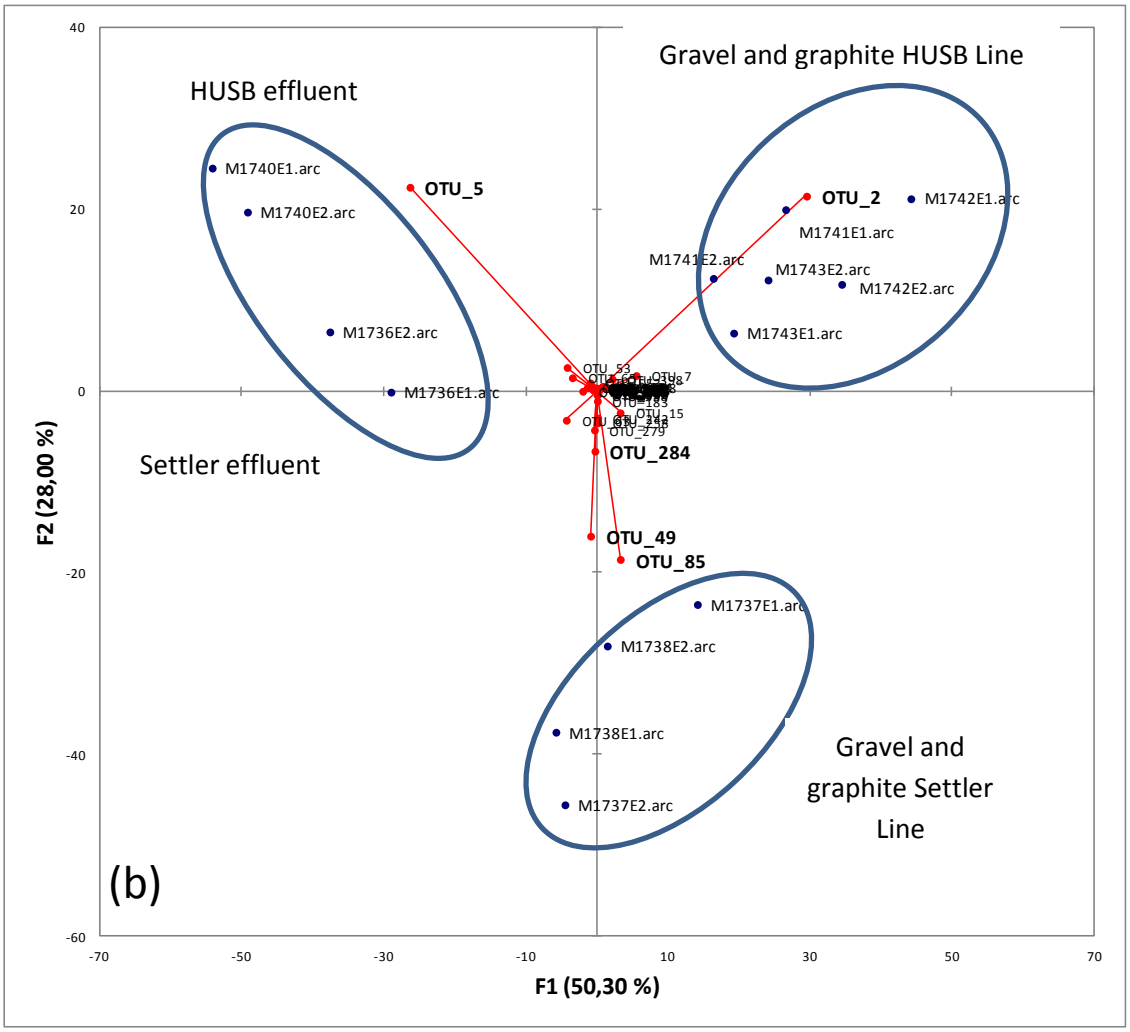

Figure 9: Covariance-based Principal Component Analysis biplot of a) eubacterial and b) archaeal OTUs distribution from pyrosequencing analysis from different samples.